Journal of Thermal Analysis and Calorimetry (2022) 147:8765–8777
https://doi.org/10.1007/s10973-021-11164-9

Ball-milled valsartan and its combination with mannitol: the case of drug polyamorphism

Iára Cristina Schmücker Lenschow[1] · Giovana Carolina Bazzo[3] · Melissa Zétola[2] · Hellen Karine Stulzer[3,4] · Luciano Soares[1,4] · Bianca Ramos Pezzini[3,4]

Received: 29 June 2021 / Accepted: 18 November 2021 / Published online: 5 January 2022

Abstract

Valsartan (VAL) is a drug that has low water solubility and low oral bioavailability. Unlike most drugs, bulk VAL has unusual solid-state properties, including the phenomenon of polyamorphism. Furthermore, surprisingly, obtaining the neat VAL in a completely amorphous form does not increase its solubility. In this study, the influence of different ball milling conditions (milling time and speed) on dissolution rate, thermoanalytical and solid-state properties of VAL was studied. The influence of the association of VAL with the hydrophilic carrier mannitol (as physical mixtures and solid dispersions, at different drug/carrier ratios) on drug dissolution, thermoanalytical and solid-state properties was also evaluated. Bulk VAL, milled-VAL and physical mixtures and solid dispersions (SDs) of the drug with mannitol were characterized by differential scanning calorimetry, powder X-ray diffraction analysis and Fourier transformed infrared spectroscopy. Ball milling the neat drug originated self-agglomerated particles, with lower dissolution rate than bulk VAL, and the conversion of VAL from a more ordered amorphous form to another fully amorphous and less soluble form. The same conversion occurred after ball milling of VAL with mannitol (SDs). This change in VAL polyamorphic forms resulting from the ball-milling process had not yet been described in other studies. The highest proportion of mannitol tested (VAL: mannitol 1:3 m/m) promoted a greater increase in the dissolution rate of the drug. A physical mixture prepared in the same composition showed a dissolution profile similar to these SDs. These results demonstrated that the simple association of VAL with mannitol is sufficient to improve its dissolution rate, without changing the solid state of drug.

Keywords Valsartan · Mannitol · Solid dispersion · Ball milling · Dissolution · Solid state

Introduction

Valsartan (VAL) is an angiotensin II antagonist used to treat hypertension and other cardiovascular diseases. It is a class II drug (low solubility and high permeability) according to the Biopharmaceutical Classification System (BCS). It has low oral bioavailability (~23%) probably related to its poor water solubility, especially in low pH conditions [1–3]. That is why many formulation approaches have been reported aiming to improve the aqueous solubility and oral bioavailability of VAL, including β-cyclodextrin complexes [4], mucoadhesive pellets [5], micro- and nanoparticles [6, 7], mesoporous silica nanoparticles [8], coamorphous systems [9], and solid dispersions [1, 3, 10, 11].

There are different reports in the literature about the unusual and very original solid-state properties of bulk VAL. Skotnicki and co-workers reported that bulk VAL was marketed in an amorphous form. The authors also suggested the existence of two amorphous forms, and thus a polyamorphic situation, that is, the possible existence of two or more distinct amorphous forms of the same compound separated by a clear phase transition. They described two VAL amorphous forms, called AR (commercial form) and AM (obtained in laboratory by heating above 100 °C and cooling). According

✉ Bianca Ramos Pezzini
bianca.pezzini@ufsc.br

1 Programa de Pós-Graduação em Saúde e Meio Ambiente, Universidade da Região de Joinville, Joinville 89219-710, Brazil

2 Departamento de Farmácia, Universidade da Região de Joinville, Joinville 89219-710, Brazil

3 Programa de Pós-Graduação em Farmácia, Universidade Federal de Santa Catarina, Florianópolis 88040-970, Brazil

4 Pharmaceutical Sciences Department, Federal University of Santa Catarina, Florianópolis 88040-970, Brazil

to these authors, the AR form, although amorphous, is characterized by presenting an expressively greater level of structural arrangement in relation to AM. The authors also reported that the AR form, surprisingly, has a higher dissolution rate than the AM form [12, 13]. The amorphous form of bulk VAL was also reported by Moura Ramos and Diogo [14]. Guinet and co-workers suggested another situation and said that the AR form of VAL is not amorphous, but a crystalline mesophase composed of nano-domains [15]. Others authors reported the crystalline state of VAL [2, 3, 8].

Solid dispersions (SDs) are a promising system to improve the aqueous solubility and the dissolution rate of drugs. Numerous works report the use of different carriers and preparation methods to obtain SDs with improved aqueous solubility and dissolution rate for many drugs, including VAL. VAL-SDs with poloxamer adsorbed on hydrophilic silica (Aeroperl® 300/30) showed a better dissolution profile than the bulk VAL in simulated gastric fluid [2]. VAL-SDs with an inorganic (calcium carbonate) and organic base (N-methyl-D-glucamine) increased the aqueous solubility and dissolution rate of the drug in simulated intestinal fluid [1]. SDs-microparticles containing VAL and Eudragit® E PO significantly improved the drug dissolution rate at pH 1.2 and pH 4.0 [3].

SDs can be prepared by several techniques such as solvent evaporation (including spray drying, supercritical fluid and co-precipitation); melting methods (like hot-melt extrusion and melting/cooling); kneading methods (including ball milling), among others [16]. Milling is a mechanical process, commonly used in the pharmaceutical field to reduce the particle size of drugs and, also, to prepare SDs. Milling can increase the dissolution rate of drugs by mechanisms such as changes in size, specific surface area and particle shape, as well as amorphization and/or structural disorder of the powder crystals [17]. Milling the drug with a hydrophilic polymer often promotes an improvement in drug solubility and minimizes the possibility of drug particles self-aggregation. Ball milling has been applied to prepare SDs due to the simplicity of the process and the non-use of organic solvents or heat [1, 18]. So, milling is a simple, environmentally friendly and cost-effective alternative to improve drugs aqueous solubility and dissolution rate [1, 19].

In this work, the influence of different ball milling conditions on the dissolution profile, thermoanalytical and solid-state properties of VAL was studied. The focus was to evaluate if the ball-milling technique could promote polyamorphic transformations of VAL and, consequently, affect its dissolution rate. In addition, the use of mannitol as a hydrophilic carrier has been evaluated to prepare physical mixtures and SDs with VAL. Mannitol is a carbohydrate of natural origin, widely used as water-soluble hydrophilic carrier for the preparation of SDs [20]. The influence of ball-milling process conditions in the presence of mannitol on the solid-state properties of VAL was also studied, as well as the impact on drug dissolution rate.

Experimental

Materials

Bulk VAL was purchased from Pharma Nostra (Campinas, SP, Brasil) and mannitol from Henrifarma Produtos Químicos e Farmacêuticos (São Paulo, SP, Brasil). All other chemicals used were of analytical grade.

Preparation of milled-VAL, SDs and physical mixtures with mannitol

Milled-VAL and VAL-mannitol SDs were prepared in a ball mill (Retsch PM 200, Germany) with two 125 mL jars, containing three 20-mm-steel balls each.

Milled-VAL was obtained using different milling times (2 or 4 h) and milling speeds (360 or 560 rpm) and was denominated as M-VAL$_{(2–360)}$, M-VAL$_{(4–360)}$, M-VAL$_{(2–560)}$, and M-VAL$_{(4–560)}$.

The SDs (6 g each) were prepared using the same conditions (milling time and milling speed) described for ball-milled-VAL and VAL/mannitol ratios of 1:1 and 1:3 (m/m) (Table 1).

VAL-mannitol physical mixtures at the ratios of 1:1 and 1:3 (m/m) (PM$_{1:1}$ and PM$_{1:3}$) were prepared by mixing the components in porcelain mortar, with the aid of a spatula.

All the samples were packed in closed amber glass flasks and stored in a desiccator for further analysis.

Dissolution study

The dissolution profiles ($n = 6$) were obtained in a dissolution tester (Nova Ética 299/6, Brazil), using the paddle apparatus (50 rpm), 1000 mL of phosphate buffer pH 6.8

Table 1 VAL-mannitol SDs prepared by ball milling

Formulation	VAL/manitol (m/m) ratio	Milling time/h	Milling speed/ rpm
SD1	1:1	2	360
SD2	1:3	2	360
SD3	1:1	4	360
SD4	1:3	4	360
SD5	1:1	2	560
SD6	1:3	2	560
SD7	1:1	4	560
SD8	1:3	4	560

at 37 ± 0.5 °C, without medium replacement. Hard gelatin capsules containing the samples equivalent to 160 mg of drug were tested using spiral sinkers. Aliquots were withdrawn at predefined time intervals, centrifuged at 3000 rpm for 15 min (Nova Técnica FC0G-0035 centrifuge, Brazil) and quantified by spectrophotometry at 250 nm (Shimadzu 1601PC spectrophotometer, Tokyo, Japan) using a previously validated methodology.

Results of the percentage of drug dissolved in 60 min (Q_{60min}) were compared by one-way ANOVA with Tukey's post hoc analysis at a p value of 0.05 (GraphPad Prism 6.01, the USA).

Differential scanning calorimetry (DSC)

DSC curves were obtained using hermetically sealed aluminum crucibles, ~ 3 mg of sample, at nitrogen atmosphere (50 mL min^{-1}) and heating (or cooling) rate of 10 °C min^{-1} (TA Instruments DSC Q20 calorimeter, the USA). For bulk VAL, the sample was initially heated from 25 to 140 °C. Next, it was cooled down to room temperature and reheated to 140 °C in a second run. Some samples were submitted to a previous treatment before DSC analysis, as described in Table 2. The equipment was calibrated with indium (T_f = 156.6 °C, ΔH_{fus} = 28.54 J g^{-1}) and zinc (T_f = 419.6 °C) before analyses.

X-ray powder diffraction (XRPD)

XRPD analyses were performed using a θ–θ X-ray diffractometer (D2 Phaser, Bruker, the USA), operating with Kα copper radiation (λ = 1.5418 Å), with current of 10 mA and voltage of 30 kV. Detection was performed on a scintillation counter one-dimensional LYNXEYE detector. Measurements were taken at room temperature, at 2θ scanning from 5° to 40° and with a 0.091° step size.

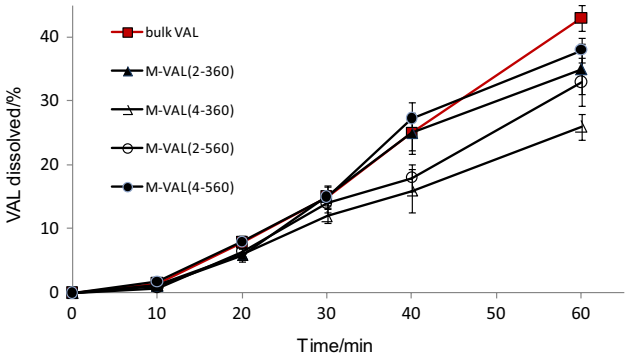

Fig. 1 Dissolution profiles of bulk VAL and milled-VAL (M-VAL) obtained under different conditions (2 or 4 h; 360 or 560 rpm)

Fourier transformed infrared spectroscopy (FTIR)

FTIR spectra were acquired on a PerkinElmer Frontier spectrophotometer (PerkinElmer, Massachusetts, the USA), using an attenuated total reflectance accessory, with the collection of 12 scans in 600–4000 cm^{-1} region at a resolution of 2 cm^{-1}.

Scanning electron microscopy (SEM)

Samples mounted onto metal stubs were vacuum-coated with gold (Denton Vaccum Desk V, Japan) and analyzed using a scanning electron microscope (Jeol JSM 6701F, Japan), operated at 15 kV.

Results and discussion

Dissolution study of bulk and ball-milled-VAL

The dissolution profiles of bulk VAL and ball-milled-VAL, obtained under different conditions (milling of 2 or 4 h; 360 or 560 rpm), are shown in Fig. 1.

Table 2 Pre-treatment performed on some samples of VAL for further analysis by DSC

Sample	Treatment	Sample denomination after treatment
Bulk VAL	Desiccation at 50 °C for 12 h	VAL-desiccated
VAL-desiccated	Direct exposure to the environment (21 °C and 73% RH**) for 24 h	VAL-moistened
$M\text{-}VAL_{(2–360)}$	Desiccation at 50 °C for 12 h	$M\text{-}VAL_{(2–360)}$-desiccated
$M\text{-}VAL_{(4–560)}$	Desiccation at 50 °C for 12 h	$M\text{-}VAL_{(4–560)}$-desiccated
$M\text{-}VAL_{(2–360)}$ desiccated	Direct exposure to the environment (21 °C and 80% RH) for 12 h	$M\text{-}VAL_{(2–360)}$-moistened
$M\text{-}VAL_{(4–560)}$ desiccated	Direct exposure to the environment (21 °C and 80% RH) for 12 h	$M\text{-}VAL_{(4–560)}$-moistened

*Desiccation performed in an air circulating oven (Lawes, Brazil)

**Relative humidity (determined with thermohygrometer)

VAL exhibits pH-dependent solubility. It is an acid drug and, therefore, is highly soluble at pH > 5.0, but poorly soluble in acidic and non-buffered solutions [3, 8, 11]. However, even in phosphate buffer pH 6.8, bulk VAL presented low dissolution (Fig. 1, ~45% of drug release in 60 min). Similar results were reported by Xu and co-workers for bulk VAL [10]. Ball milling under different conditions of time (2 or 4 h) and speed (360 or 560 rpm) did not result in improvement of VAL dissolution profile. On the contrary, Q_{60min} values of all milled-VAL samples were lower than bulk drug ($p < 0.05$).

Milling is a process that can be used to increase drugs dissolution rate. The mechanisms by which milling enhances drug dissolution include alterations in the size, specific surface area and shape of the drug particles as well as milling-induced amorphization and/or structural disordering of the drug crystal (mechanochemical activation) [17]. However, in this study, ball milling of VAL did not prove to be an efficient process to improve its dissolution rate. In the SEM micrographs of VAL before and after the mechanical treatment using different milling conditions (Fig. 2), it is evident that VAL particles self-agglomerated, with an increase in

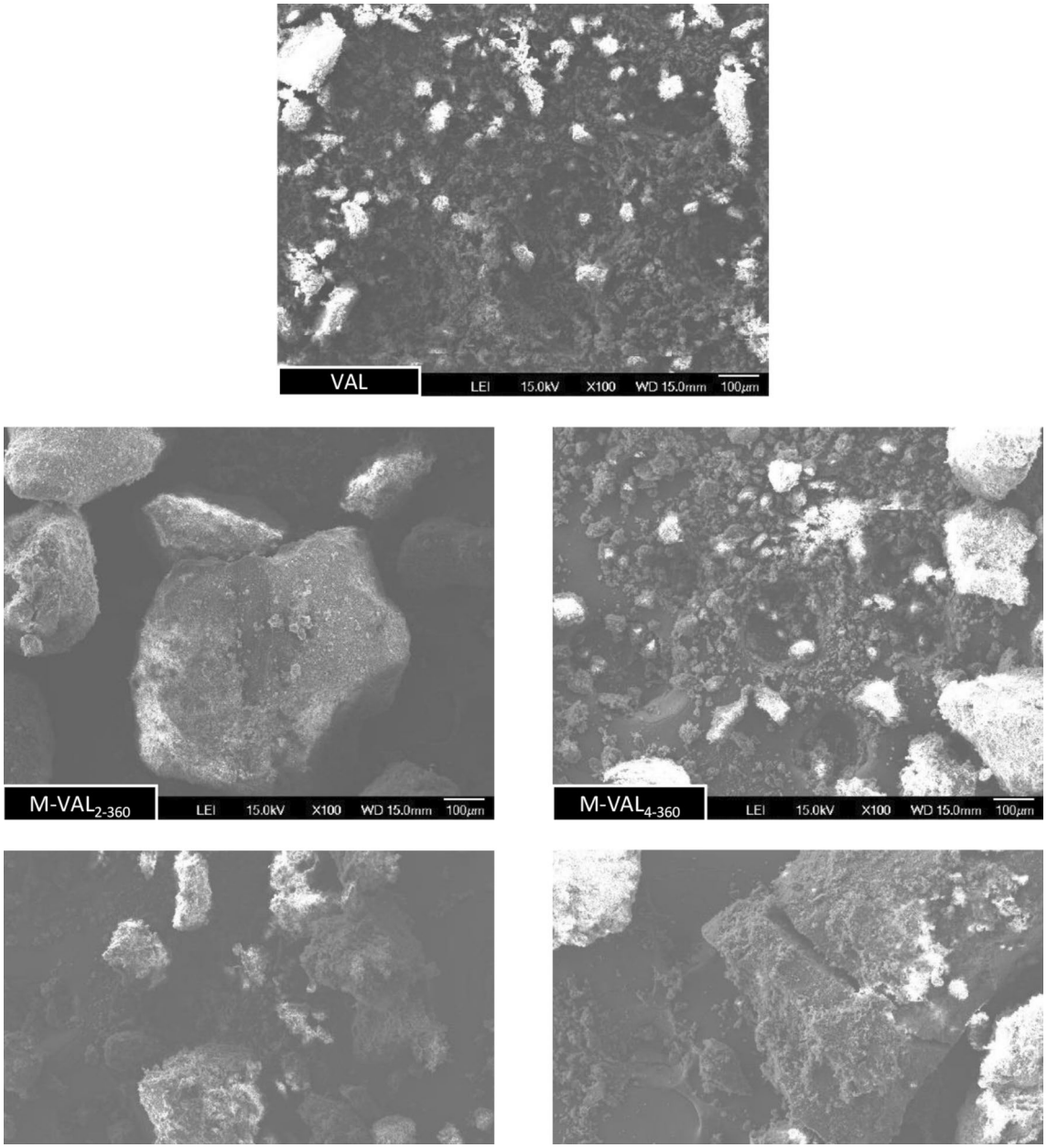

Fig. 2 SEM of bulk valsartan (VAL) and milled-VAL (M-VAL) obtained under different conditions (2 or 4 h; 360 or 560 rpm) (magnification of 100×)

particle size induced by the milling process, which is one of the factors that may have influenced the decrease in drug dissolution rate. Xu and co-workers also observed that the treatment of VAL in a planetary mill did not significantly enhance its aqueous dissolution, and some decrease occurred probably due to the self-aggregation of VAL particles that resulted from the strong direct pressure and shearing force created by the high acceleration of grinding media in the planetary mill [1].

Numerous factors can affect drug dissolution, such as particle size, specific surface area, surface energy, solid-state modifications (polymorphism, polyamorphism and amorphization), type of dosage form, interaction with polymers and excipients, among others. The impact on drug dissolution may therefore be a combination of different factors. The conversion of bulk VAL to another amorphous form during the milling process is another condition that may also have influenced the drug dissolution rate, as will be discussed later.

Thermoanalytical characterization of bulk and ball-milled-VAL

Figure 3a shows the DSC curves of bulk VAL. In the first heating, two endothermic events could be observed: one at the range of 90–100 °C and other at $T_{peak} = 104$ °C ($\Delta H = 26$ J g^{-1}). Some authors attributed the endothermic peak at ~ 104 °C to the melting of crystalline VAL [8, 21]. However, other authors say that this event corresponds to a glass transition with high enthalpy relaxation peak overlapped with a change of heat capacity, since bulk VAL is not crystalline. As previously mentioned, it is reported in the literature that VAL has an unusual situation of polyamorphism and two amorphous forms of VAL are described: AR (more orderly, although amorphous) and AM (completely amorphous) [12, 13].

A small broad peak around 60–80 °C is reported for the DSC curve of bulk VAL, corresponding to a loss of water [12, 22]. In the present work, the first event in the DSC curve (Fig. 3a) occurred in a slightly higher temperature range (90–100 °C). To confirm if this event corresponded to loss of water, a new experiment was carried out, in which bulk VAL was submitted to desiccation in an oven (50 °C, 12 h) and then exposed to an environment with high relative humidity (21 °C and 73% RH, for 24 h), as described in Table 2. The DSC curves of these samples, shown in Fig. 3b, confirmed that the endothermic event in the range of 90–100 °C corresponded to the loss of water by bulk VAL.

Finally, an event was observed at 76.8 °C in the second heating of bulk VAL (Fig. 3a), corresponding to the glass transition temperature (Tg) of amorphous VAL (AM form), which can be obtained by heating the AR form until 140 °C, followed by cooling [9, 12, 22].

Samples of milled-VAL obtained under different milling conditions were also analyzed by DSC (Fig. 4), revealing changes in thermal behavior in comparison to bulk VAL. After milling, the drug presented an endothermic event with maximum between 61.20 °C (M-VAL$_{(4–560)}$) and 68.02 °C (M-VAL$_{(2–360)}$) that can be attributed to a glass transition of the AM form [12]. So, the present work is the first reporting that VAL-AM form can be obtained by milling.

The intensity of the enthalpic relaxation peak observed in the DSC curve of the AR form (bulk VAL) can be attributed to some level of VAL molecules arrangement, influenced by storage of the sample at room temperature and the presence of adsorbed water. Skotnicki et al. exposed VAL samples (AM form) to 45 °C during different time intervals and then submitted them to DSC analysis. Longer storage times caused a higher level of molecular arrangement and increased the intensity of the enthalpic relaxation peak (transition of AM form to AR form).

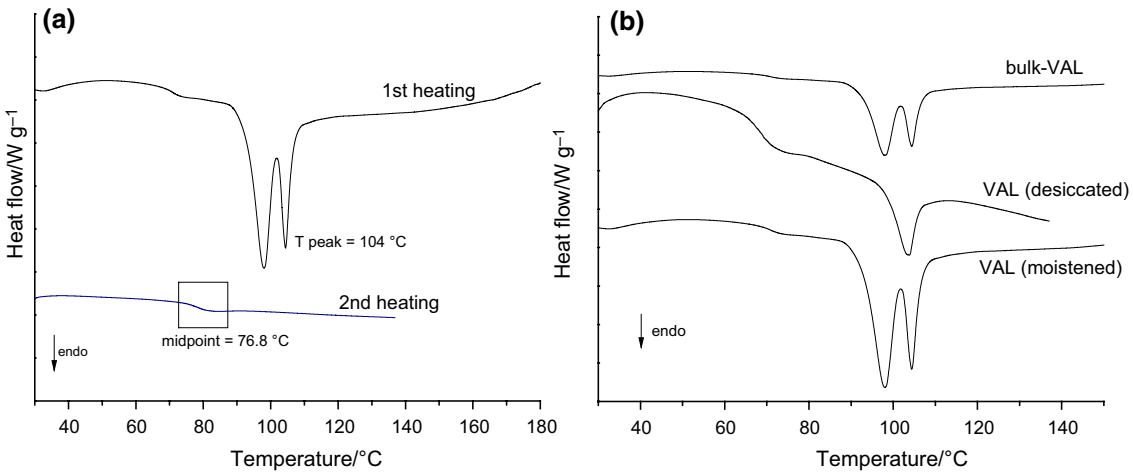

Fig. 3 DSC curves of bulk VAL **a** submitted to heating, cooling and reheating conditions; and **b** exposed to different conditions of humidity

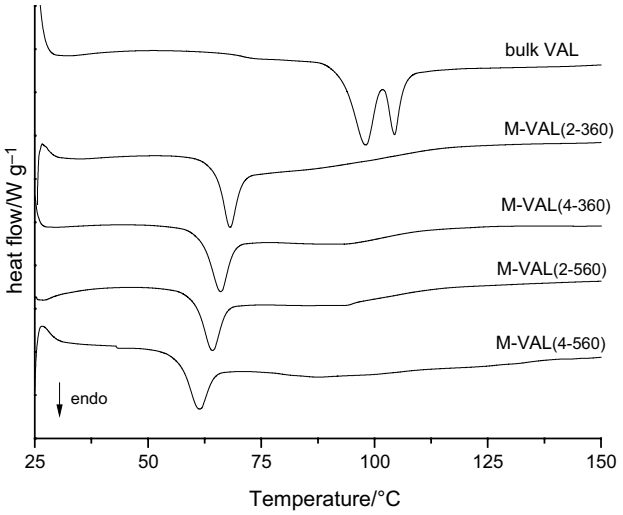

Fig. 4 DSC of bulk VAL and milled-VAL obtained under different milling conditions (2 or 4 h; 360 or 560 rpm)

New experiments were carried out to evaluate the influence of storage time and the presence of adsorbed water on the thermoanalytical properties of M-VAL samples. $M\text{-}VAL_{(2–360)}$ and $M\text{-}VAL_{(4–560)}$, corresponding to the mildest and most drastic milling conditions, were analyzed under different situations: (1) immediately after preparation; (2) immediately after drying for 12 h at 50 °C; (3) immediately after direct exposure of the desiccated samples to the high humidity environment (21 °C; 80% RH, for 12 h); and (4) 1 month after storage in a desiccator (Table 2).

For both samples, the same thermal behavior was observed in the DSC curves (Fig. 5a and b): desiccation for 12 h gave rise to an evident endothermic peak of enthalpic relaxation, at a temperature higher than the glass transition observed for the samples analyzed immediately after milling. The appearance of the structural relaxation event occurred due to physical aging for 12 h, which led to greater ordering and less molecular mobility in the samples. The effect of aging was corroborated when the desiccated samples were analyzed after 1 month of storage, since there was an increase in the intensity of the enthalpy relaxation peak, in relation to that observed in the DSC curves obtained immediately after the desiccation of the samples.

It is also possible to observe the effect of water in both moistened samples (Fig. 5a and b), which caused a reduction in the Tg, in relation to the respective desiccated samples. Additionally, the storage of the moistened samples in a desiccator for 1 month, led to the displacement of the glass transition to higher temperatures and to an increase in the intensity of the enthalpic relaxation peak. These results demonstrated the effect of physical aging on the thermal behavior of the samples. These findings are consistent with the reports by Skotnicki et al. [12] and Ramos and Diogo

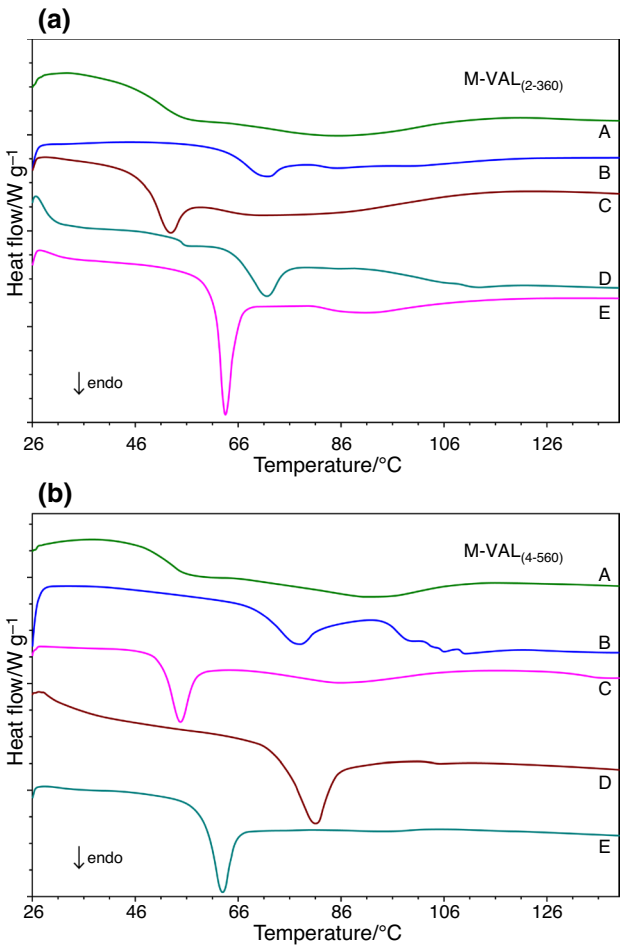

Fig. 5 DSC curves of $M\text{-}VAL_{(2–360)}$ and $M\text{-}VAL_{(4–560)}$ immediately after milling (**a**); after drying for 12 h at 50 °C (**b**); after drying and stored in a desiccator for 1 month (**c**); after direct exposure to a high humidity environment (21 °C; 80% RH) (**d**); and after exposure to high humidity conditions and stored in a desiccator for 1 month (**e**)

[17] and are additional evidence of the amorphous nature of these samples.

XRPD and FTIR of bulk and ball-milled-VAL

XRPD and FTIR are solid-state techniques that also allow to differentiate the polyamorphic forms of VAL. According to the studies of Skotnicki and co-workers, the diffraction patterns of the two amorphous forms of VAL (AR and AM) present some differences. The AR form, although amorphous, is characterized by presenting a significantly higher level of structural arrangement in relation to AM. In the diffractogram of the AR form, the authors describe a broad peak around $2\theta = 14.4°$ and a sharper peak, although small, around $2\theta = 17.3°$. The diffraction peak at $2\theta \sim 14°$ is greatly reduced for the AM form in relation to the AR. In the diffractogram of the AM form, the position of the maximum

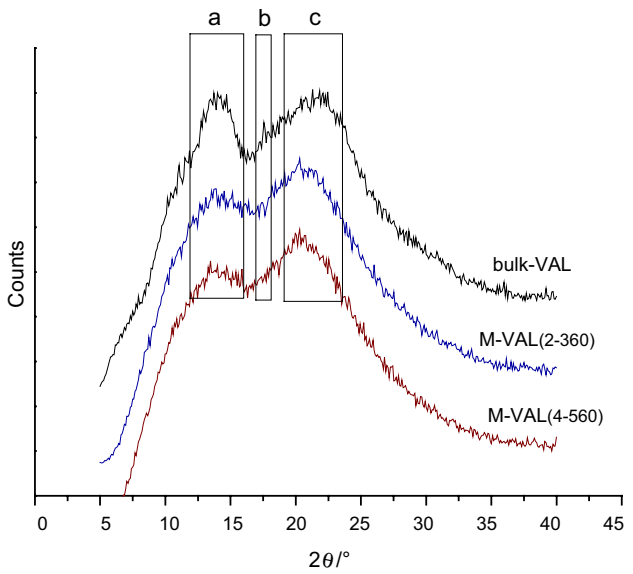

Fig. 6 Diffractograms of bulk valsartan (VAL) and milled-VAL (M-VAL) obtained under different conditions (2 or 4 h; 360 or 560 rpm)

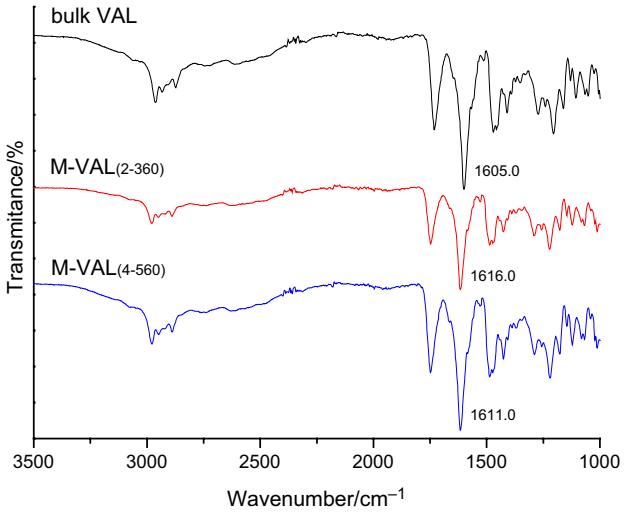

Fig. 7 FTIR spectra of bulk VAL and milled-VAL obtained under different milling conditions (M-VAL$_{(2–360)}$ and M-VAL$_{(4–560)}$)

peak occurs at $2\theta = 20.8°$, while it occurs at $2\theta = 22.3°$ in the form AR [12, 13].

In the present work, XRPD pattern of bulk VAL (Fig. 6) showed some differences in relation to those of ball-milled-VAL (M-VAL$_{(2–360)}$ and M-VAL$_{(4–560)}$). These samples were selected for analysis because they correspond to the mildest and the most drastic milling conditions.

Looking at the diffractograms shown in Fig. 6, it is clear that bulk VAL corresponds to the AR form. On the other hand, in the XRPD patterns of ball-milled-VAL, there was a shift of the maximum peak at $2\theta = 21.8°$ to 20.3° (identified with the letter "c" in Fig. 6), the disappearance of the peak at $2\theta \sim 17°$ (letter "b") and a reduction in peak intensity at $2\theta \sim 14°$ (letter "a"). These findings confirm that there was a transition of VAL from a more orderly form (AR) to another one, with lower molecular order (AM, according to Skotnicki et al.), due to mechanical activation during the milling process. The conversion of VAL from the AR to the AM form may have contributed to reduce its dissolution rate (Fig. 1). It is reported that the AR form, surprisingly, has a higher intrinsic dissolution rate than the AM form [13].

It is important to mention that there are other opinions described in the literature about the solid state of VAL. Guinet and co-workers said that the AR form is not amorphous but a crystalline mesophase. The authors obtained a glassy VAL (named as G form) by heating AR form above 100 °C and cooling down to room temperature [15]. The diffractograms presented by Guinet et al., comparing the AR form and the G form (equivalent to AM), are very similar to those obtained by Skotnicki and co-workers [12, 13]. However, Guinet et al. suggest that the peak at $2\theta = 17.7°$ is indicative of a long-range ordering, which characterizes the occurrence of a nano-crystalline state in the AR form, and that this same peak at $2\theta = 17.7°$ does not occur in the diffractogram of the G form because it is amorphous [15].

The FTIR spectra of bulk VAL and milled-VAL (M-VAL$_{(2–360)}$ and M-VAL$_{(4–560)}$), corresponding to the mildest condition (2 h, 360 rpm) and the most drastic condition (4 h, 560 rpm) of milling, are shown in Fig. 7.

The FTIR spectrum of bulk VAL corresponded to that described in the literature, with the characteristic bands at 2963 and 2873 cm^{-1} (C-H vibrations), 1738.5 cm^{-1} (carboxyl carbonyl stretching vibration), 1605 cm^{-1} (amide carbonyl stretching vibration), 1470 cm^{-1} (vibrations of C=C bonds in aromatic rings) and 938 cm^{-1} (out of plane vibrations of O–H bond in carboxylic group) [11, 23]. The band at 1605 cm^{-1} shifted to higher wave numbers for milled-VAL [1616 cm^{-1} and 1611 cm^{-1}, to M-VAL$_{(2–360)}$ and M-VAL$_{(4–560)}$, respectively]. The shift of this absorption band was also reported by Skotnicki et al. (2016) and confirms the transition from bulk VAL of the most orderly (AR form) to another less ordered (AM form), due to the milling process.

An interesting fact observed in this study was that the milling caused a change in the solid state of the bulk VAL to another less ordered form (similar to AM or G). These findings are unpublished until now since the AM (or G) form in the aforementioned studies was obtained by heating bulk VAL above 100 °C and cooling at room temperature. In the present work, this less ordered form was obtained by milling, and the temperature at the end of the process did not exceed 50.5 °C.

Thermoanalytical and solid-state characterization of physical mixtures and solid dispersions with mannitol

As demonstrated previously, the ball milling of VAL did not result in a significant improvement in the drug dissolution rate (Fig. 1). In addition, it caused particle aggregation and changes in the solid state of VAL, which contributed to decrease the drug dissolution rate. Therefore, it was decided to evaluate the effect of adding a hydrophilic carrier on dissolution and solid-state properties of VAL.

Preliminary tests were carried out to select the most suitable carrier for obtaining the SDs: sodium alginate, hydroxypropylmethylcellulose (HPMC) or mannitol. Such carriers were selected because they presented satisfactory results for obtaining SDs with other drugs [18, 24]. SDs containing VAL and each of the mentioned carriers were prepared by ball milling, and the corresponding drug dissolution profiles were evaluated (data not shown). The VAL-mannitol combination showed better drug dissolution results than the other polymers. At the end of the dissolution test, it was observed that HPMC and sodium alginate swelled and formed a gel, which probably hindered the penetration of water, impairing the dissolution of the drug. So, mannitol was chosen for preparing both SDs and physical mixtures with VAL.

DSC curves of VAL-mannitol physical mixtures showed two endothermic peaks (Fig. 8a). The first, of lower intensity and indicated in Fig. 8a, corresponds to the phase transition event described for bulk VAL ($T_{peak} = 104$ °C, $\Delta H = 26$ J g^{-1}) in Fig. 3. The second peak is related to the melting of mannitol [20, 25]. As shown in Table 3, there were no significant changes in T_{peak} values of mannitol in the physical mixtures with VAL. Furthermore, the ΔH_m values of mannitol were equivalent to its proportion in the mixture, indicating the absence of interactions. Minor changes in the melting endotherm of mixtures can occur and can be attributed to the mixing of both components, and not indicate potential incompatibility. Variations in the enthalpy values for binary mixtures can be attributed to some heterogeneity in the small samples used for the experiments [20]. The same happened with the first event, corresponding to the phase transition of VAL, without significant changes and confirming absence of interactions.

A well-defined event that can be attributed to a glass transition of the AM form was presented in the DSC curves of SD1, SD3, SD5 and SD7 (VAL:mannitol 1:1 m/m) (Fig. 8b, Table 3), in the same temperature range observed for VAL after submitted to different milling conditions (Fig. 4). This demonstrates that the change in thermal behavior observed for bulk VAL as a result of ball-milling process also occurred for these SDs. However, for SD2, SD4, SD6 and SD8, the thermal event of VAL appeared less clear, probably due to the presence of mannitol in greater quantities in these SDs [1: 3 (m/m)]. As observed for milled-VAL, DSC results suggest that there was a transition from AR form (bulk VAL) to a completely amorphous form in SDs.

All SDs presented the melting peak characteristic of mannitol (Fig. 8b). However, when comparing ΔH_m values with the corresponding physical mixture (Table 3), a decrease is observed, suggesting the amorphization of part of the mannitol. This amorphization probably occurred during the ball-milling process and could be confirmed by XRPD analyses.

Figure 9 shows the diffractograms of SD2, SD8 and $PM_{1:3}$. The analysis of these samples was chosen, since they were the formulations with the best performance in the dissolution study, as will be demonstrated later.

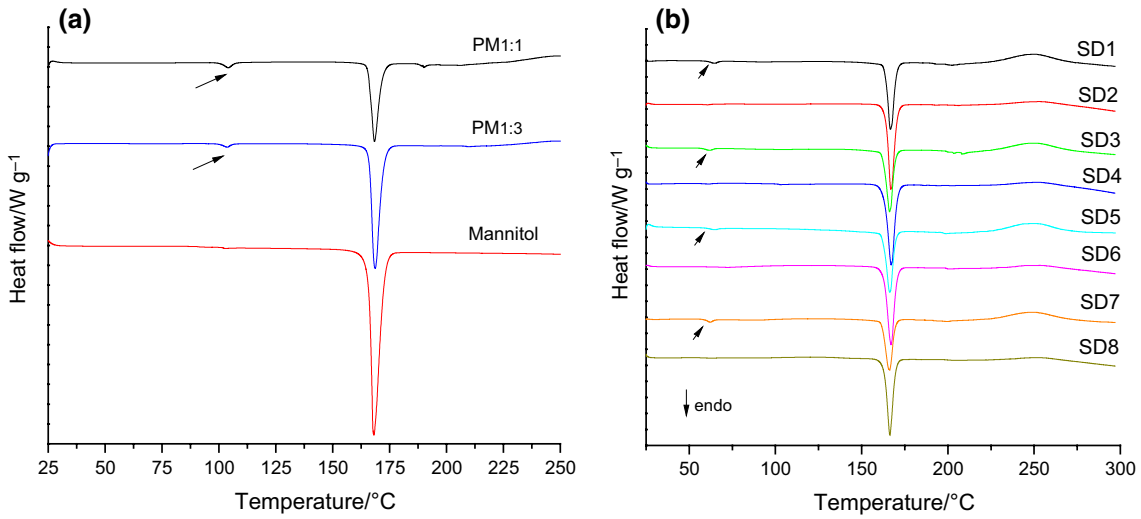

Fig. 8 DSC curves of mannitol and physical mixtures of VAL/mannitol at 1:1 and 1:3 m/m ratio ($PM_{1:1}$ and $PM_{1:3}$) (**a**); and solid dispersions (SD1 to SD8) (**b**)

Table 3 Temperature and enthalpy (ΔH) values for mannitol, physical mixtures ($PM_{1:1}$ and $PM_{1:3}$) and solid dispersions (SD1 to SD8). DSC curves are shown in Fig. 8

Sample	VAL events		mannitol events	
	1st peak (T_{peak})/°C	1st peak (ΔH)/Jg^{-1}	2nd peak (T_{peak})/°C	2nd peak (ΔH_m)/Jg^{-1}
$PM_{1:1}$	104.1	12.3	167.3	143.5
$PM_{1:3}$	103.6	8.2	167.6	183.9
Mannitol	–	–	167.1	284.9
	1st event (Tg)/°C		2nd peak (T_{peak})/°C	2nd peak (ΔH_m)/Jg^{-1}
SD1	64.7		166.6	99.5
SD2	ND		166.9	120.6
SD3	61.3		166.2	95.0
SD4	ND		167.1	132.1
SD5	63.3		166.3	100.5
SD6	ND		167.0	122.1
SD7	60.7		166.2	97.7
SD8	ND		166.3	107.7

ND = not detected

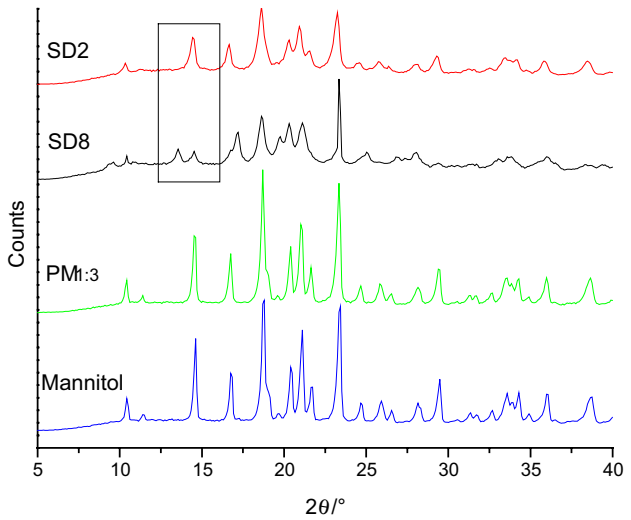

Fig. 9 Diffractograms of solid dispersions (SD2 and SD8), physical mixture of VAL:mannitol ($PM_{1:3}$) and mannitol

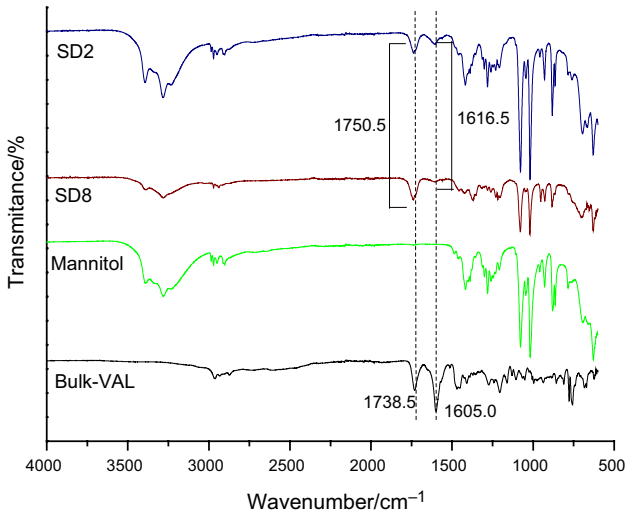

Fig. 10 FTIR spectra of bulk VAL, mannitol and solid dispersions (SD2 and SD8)

Mannitol has a crystalline structure (characteristic reflections at 10.5°, 14.7°, 16.5°, 18.8°, 20.5° and 23.4°), compatible with its polymorphic form β [20, 25].

The XRPD pattern of $PM_{1:3}$ was similar to that presented by mannitol, as expected, since this was the component in greater quantity in the sample. The lower intensity of reflections observed for SD2 and SD8, in comparison with $PM_{1:3}$ (same drug/carrier ratio), suggested the amorphization of part of the mannitol present in these SDs, corroborating the DSC results.

SD2 and SD8 showed different diffraction patterns, as indicated in Fig. 9. The diffractogram of SD2 was similar to that of mannitol, showing that this SD contained the same polymorphic form (β) of the carrier. On the other hand, SD8 presented a different pattern, indicating the conversion of mannitol from β to α polymorphic form [25, 26], probably due to the more drastic milling conditions used to prepare

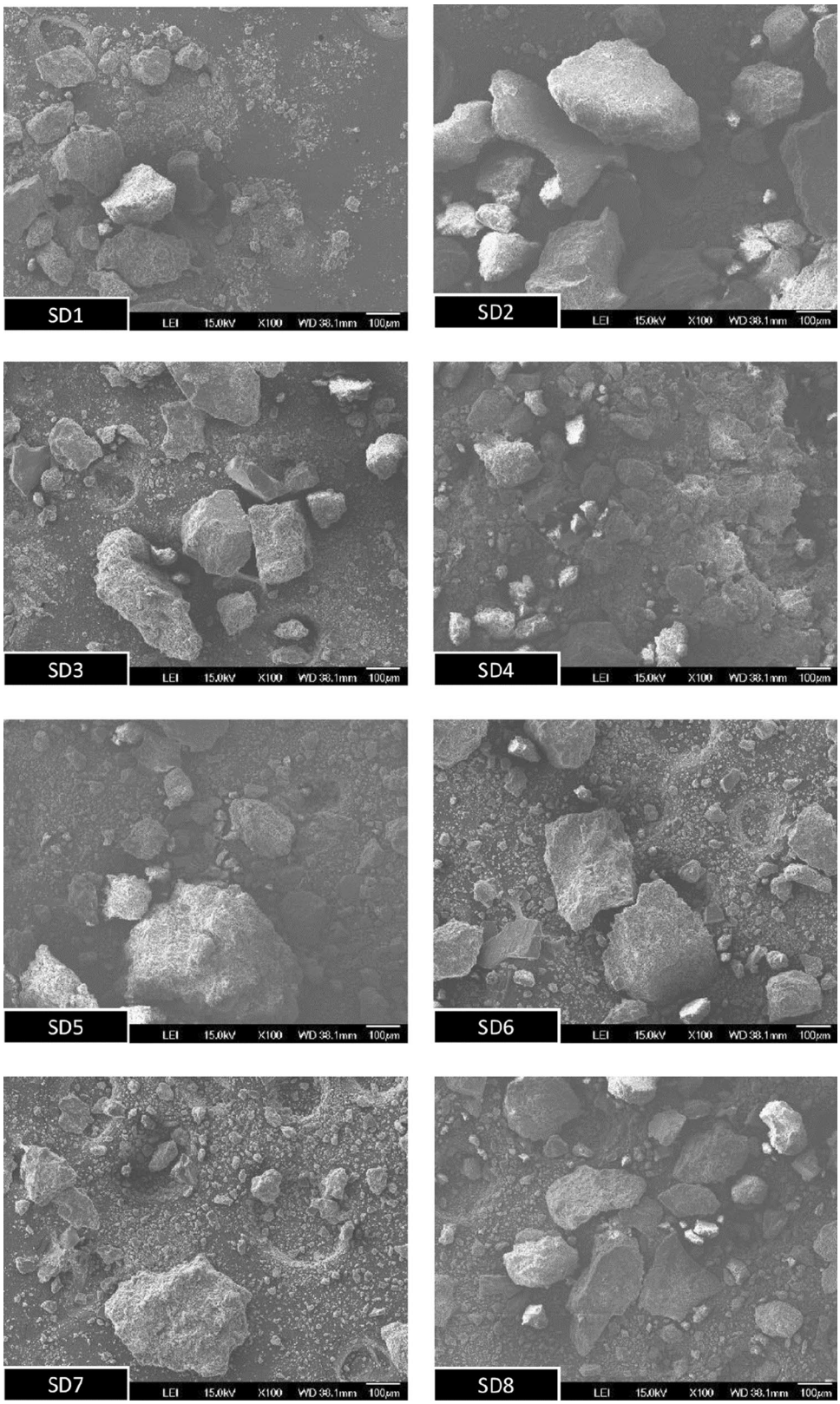

Fig. 11 SEM of solid dispersions (SD1 to SD8) (magnification of 100×)

this SD. The results were confirmed by FTIR (Fig. 10). The comparison of FTIR spectra with data from the literature [25, 26] confirmed the presence of mannitol β polymorphic form in SD2 and α polymorphic form in SD8.

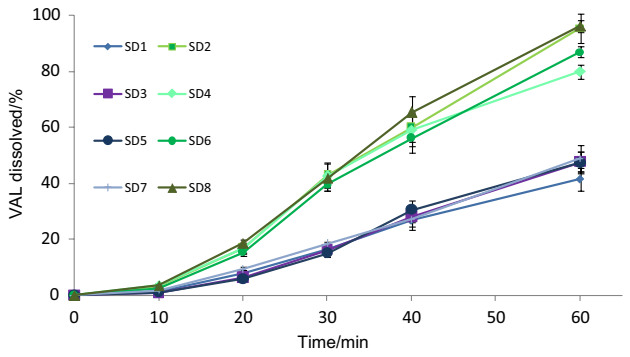

Fig. 12 Dissolution profiles of solid dispersions (SD1 to SD8) prepared with different VAL/mannitol ratios (1:1 or 1:3 m/m) and obtained under different milling conditions (2 or 4 h; 360 or 560 rpm)

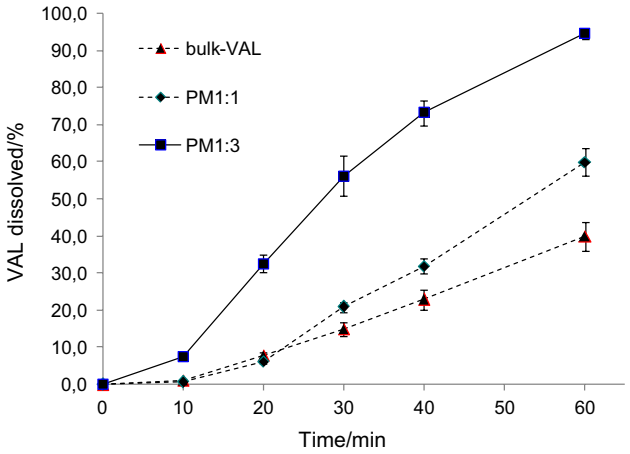

Fig. 13 Dissolution profiles of bulk VAL and physical mixtures with mannitol in the proportions of 1:1 and 1:3 (m/m) ($PM_{1:1}$ and $PM_{1:3}$)

In the diffractograms of the SDs, it was not possible to observe the characteristic peaks of VAL (form AR or AM) due to the presence of the high-intensity peaks of mannitol. However, in Fig. 10, it is possible to see that the bands at 1605 cm^{-1} and 1738.5 cm^{-1}, observed in the bulk VAL FTIR spectrum, shifted to higher wave numbers in the SD2 and SD8 spectra, as observed for VAL submitted to different milling conditions, indicating the presence of the amorphous form AM (or G) of VAL in the SD2 and SD8, as suggested by DSC analyses.

All SDs demonstrated morphological alterations when compared to the bulk drug, presenting as VAL-mannitol agglomerates with irregular shape (Fig. 11). Similar results have been reported for SDs prepared by ball-milling process [18, 26]. Ball milling of VAL in the absence of the hydrophilic carrier also caused agglomeration of the particles (Fig. 2), being one of the factors that may have contributed to decrease the drug dissolution rate, together with the polyamorphic conversion. However, in the case of SDs, the occurrence of these aggregates does not seem to have significantly affected the dissolution of VAL. For example, SDs prepared with a higher amount of mannitol (SDs 2, 4, 6 and 8) showed a higher dissolution rate than the neat drug, as will be discussed below. In this case, the high solubility of mannitol in the aqueous medium must have promoted the rapid solubilization of these aggregates. The co-milling of poorly water-soluble drugs with hydrophilic carriers can increase wettability, bringing advantages in terms of solubility [24, 27].

Dissolution study of VAL solid dispersions and physical mixtures with mannitol

The dissolution profiles of solid dispersions are shown in Fig. 12. SDs prepared with VAL/mannitol ratio of 1:1 (m/m), obtained with different speeds and milling times, presented similar dissolution profiles and similar Q_{60min}values ($p > 0.05$) in relation to bulk VAL. This shows that for the 1:1 (m/m) ratio, under the conditions tested, milling with mannitol did not influence the dissolution rate of VAL.

All SDs prepared with VAL/mannitol ratio of 1:3 (m/m) had higher dissolution profiles and higher Q_{60min} values ($p < 0.001$) compared to bulk drug showing that in this proportion, the SDs were efficient in improving the dissolution rate of VAL.

The best dissolution results were achieved for SD2 (2 h; 360 rpm) and SD8 (4 h; 560 rpm) formulations, both containing VAL:mannitol in the proportion of 1:3 (m/m), with approximately 90% of drug dissolved in 60 min. The Q_{60min}values of SD2 and SD8 showed no significant difference between them ($p > 0.05$) and were superior in relation to all other SDs ($p < 0.01$) presented in Fig. 12.

When observing the improvement of the dissolution profile of a drug from a SD, it is essential to verify if the effect was the result of obtaining the SD itself (use of a specific carrier associated with the drug and a process for obtaining the SD) or if the performance observed was due only to the presence of the carrier. For that, it was necessary to compare the dissolution profiles of the SDs with those obtained for physical mixtures [PM] (simple mixtures between the drug and the carrier) with same composition of the respective SDs, but not subjected to the milling process. The dissolution profiles of physical mixtures of VAL/mannitol at the ratios of 1:1 and 1:3 (m/m) (named as $PM_{1:1}$ and $PM_{1:3}$) are shown in Fig. 13.

$PM_{1:1}$ and $PM_{1:3}$ promoted an improvement in the dissolution profile of VAL, presenting higher values of Q_{60min} ($p < 0.001$) compared to the bulk drug. The Q_{60min}value of $PM_{1:3}$ ($94.5 \pm 1.3\%$) was equivalent to those obtained for SD2 ($90.0 \pm 4.9\%$) and SD8 ($88.5 \pm 6.9\%$) ($p > 0.05$). The

dissolution profiles of $PM_{1:1}$ and $PM_{1:3}$ demonstrate that the simple association of VAL with mannitol has a positive effect on drug dissolution rate and may be sufficient to improve the dissolution performance when an adequate drug/carrier ratio is used.

Another fact to be considered is the conversion of VAL to AM form in SDs, which has a lower dissolution rate than the AR form [13, 15]. This phenomenon helps to explain why the dissolution performance of $PM_{1:3}$ was better than that of SD2 and SD8, although the Q_{60min} results showed a statistically significant similarity, since the physical mixture contained the AR form of VAL, while the SDs (2 and 8) contained the less soluble AM form.

Conclusions

Most of the active pharmaceutical ingredients are in the crystalline form and, after conversion to amorphous form, have their solubility and/or dissolution rate improved. However, in this study, unusual thermoanalytical, solid-state and dissolution properties were evidenced for VAL, as well for its physical mixtures and SDs with mannitol.

The ball-milling of VAL, under different process conditions, led to changes in its solid state and, also, to a decrease in its dissolution rate. The self-aggregation of the neat drug particles and the conversion of VAL from an amorphous form with greater level of structural arrangement to a completely amorphous and surprisingly less soluble form have contributed to the decrease of the drug dissolved amount.

The preparation of ball-milled SDs with mannitol also caused a change in the solid state of VAL, originating a less ordered amorphous form. The proportion of mannitol present in SD formulations significantly affected the dissolution of VAL. The highest proportion promoted a greater increase in the dissolution rate of the drug. However, the physical mixture prepared in the same composition showed a dissolution profile similar to the SDs. These results demonstrated that the simple association of VAL with mannitol may be sufficient to improve its dissolution rate and do not cause changes in the solid state of bulk VAL.

Author contributions ICSL was involved in conceptualization, methodology, investigation, writing; GCB contributed to methodology, writing; MZ and LS were involved in methodology, investigation; HKS contributed to investigation, writing; BR was involved in conceptualization, investigation, writing, supervision.

Funding Iára Cristina Schmücker Lenschow is thankful to Coodenação de Aperfeiçoamento de Pessoal de Nível Superior for her graduate studies fellowship (CAPES-DS, Brazil).

Declarations

Conflicts of interest The authors declare that they have no conflict of interest.

References

1. Xu W, Sun Y, Du L, Chistyachenko YS, Dushkin AV, Su W. Investigations on solid dispersions of valsartan with alkalizing agents: Preparation, characterization and physicochemical properties. J Drug Deliv Sci Technol. 2018;44:399–405.
2. Park J-B, Park C, Piao ZZ, Amin HH, Meghani NM, Tran PHL, et al. pH-independent controlled release tablets containing nanonizing valsartan solid dispersions for less variable bioavailability in humans. J Drug Deliv Sci Technol. 2018;46:365–77.
3. Pradhan R, Kim SY, Yong CS, Kim JO. Preparation and characterization of spray-dried valsartan-loaded Eudragit® E PO solid dispersion microparticles. Asian J Pharm Sci. 2016;11:744–50.
4. Chadha R, Bala M, Arora P, Jain DVS, Pissurlenkar RRS, Coutinho EC. Valsartan inclusion by methyl-β-cyclodextrin: thermodynamics, molecular modelling, Tween 80 effect and evaluation. Carbohydr Polym. 2014;103:300.
5. Cao Q-R, Liu Y, Xu W-J, Lee B-J, Yang M, Cui J-H. Enhanced oral bioavailability of novel mucoadhesive pellets containing valsartan prepared by a dry powder-coating technique. Int J Pharm. 2012;434:325–33.
6. Ma Q, Sun H, Che E, Zheng X, Jiang T, Sun C, et al. Uniform nano-sized valsartan for dissolution and bioavailability enhancement: Influence of particle size and crystalline state. Int J Pharm. 2013;441:75–81.
7. Kumar A, Davern P, Hodnett BK, Hudson SP. Carrier particle mediated stabilization and isolation of valsartan nanoparticles. Colloids Surf B Biointerfaces. 2019;175:554–63.
8. Biswas N. Modified mesoporous silica nanoparticles for enhancing oral bioavailability and antihypertensive activity of poorly water soluble valsartan. Eur J Pharm Sci. 2017;99:152–60.
9. Lodagekar A, Chavan RB, Mannava MKC, Yadav B, Chella N, Nangia AK, et al. Co amorphous valsartan nifedipine system: Preparation, characterization, in vitro and in vivo evaluation. Eur J Pharm Sci. 2019;139:105048.
10. Xu W-J, Xie H-J, Cao Q-R, Shi L-L, Cao Y, Zhu X-Y, et al. Enhanced dissolution and oral bioavailability of valsartan solid dispersions prepared by a freeze-drying technique using hydrophilic polymers. Drug Deliv. 2016;23:41–8.
11. Medarević D, Cvijić S, Dobričić V, Mitrić M, Djuriš J, Ibrić S. Assessing the potential of solid dispersions to improve dissolution rate and bioavailability of valsartan: In vitro-in silico approach. Eur J Pharm Sci. 2018;124:188–98.
12. Skotnicki M, Gaweł A, Cebe P, Pyda M. Thermal behavior and phase identification of Valsartan by standard and temperature-modulated differential scanning calorimetry. Drug Dev Ind Pharm. 2013;39:1508–14.
13. Skotnicki M, Apperley DC, Aguilar JA, Milanowski B, Pyda M, Hodgkinson P. Characterization of two distinct amorphous forms of valsartan by Solid-State NMR. Mol Pharm. 2016;13:211–22.
14. Moura Ramos JJ, Diogo HP. Thermal behavior and molecular mobility in the glassy state of three anti-hypertensive pharmaceutical ingredients. RSC Adv. 2017;7:10831–40.
15. Guinet Y, Paccou L, Danède F, Derollez P, Hédoux A. Structural description of the marketed form of valsartan: A crystalline mesophase characterized by nanocrystals and conformational disorder. Int J Pharm. 2017;526:209–16.

16. Tran P, Pyo YC, Kim DH, Lee SE, Kim JK, Park JS. Overview of the manufacturing methods of solid dispersion technology for improving the solubility of poorly water-soluble drugs and application to anticancer drugs. Pharmaceutics. 2019;11:1–26.
17. Loh ZH, Samanta AK, Sia Heng PW. Overview of milling techniques for improving the solubility of poorly water-soluble drugs. Asian J Pharm Sci. 2015;10:255–74.
18. Nart V, França MT, Anzilaggo D, Riekes MK, Kratz JM, De Campos CEM, et al. Ball-milled solid dispersions of BCS Class IV drugs: Impact on the dissolution rate and intestinal permeability of acyclovir. Mater Sci Eng C. 2015;53:229–38.
19. Zhong L, Zhu X, Luo X, Su W. Dissolution properties and physical characterization of telmisartan-chitosan solid dispersions prepared by mechanochemical activation. AAPS Pharm Sci Tech. 2013;14:541–50.
20. Han Y, Faudone S, Zitto G, Bonafede S, Rosasco M, Segall A. Physicochemical characterization of physical mixture and solid dispersion of diclofenac potassium with mannitol. J Appl Pharm Sci. 2017;7:204–8.
21. Patel DM, Patel DJ, Shah SK, Shah AS. Formulation and evaluation of fast dissolving tablets of nebivovol and valsartan. Res J Pharm Technol. 2020;11:5530–9.
22. Skotnicki M, Aguilar JA, Pyda M, Hodgkinson P. Bisoprolol and bisoprolol-valsartan compatibility studied by differential scanning calorimetry, nuclear magnetic resonance and X-Ray powder diffractometry. Pharm Res. 2015;32:414–29.
23. Ha NS, Tran TT-D, Tran PH-L, Park J-B, Lee B-J. Dissolution-enhancing mechanism of alkalizers in poloxamer-based solid dispersions and physical mixtures containing poorly water-soluble valsartan. Chem Pharm Bull (Tokyo). 2011;59:844–50.
24. Cares-Pacheco MG, Vaca-Medina G, Calvet R, Espitalier F, Letourneau J-J, Rouilly A, et al. Physicochemical characterization of d-mannitol polymorphs: The challenging surface energy determination by inverse gas chromatography in the infinite dilution region. Int J Pharm. 2014;475:69–81.
25. Burger A, Henck J-O, Hetz S, Rollinger JM, Weissnicht AA, Stöttner H. Energy/temperature diagram and compression behavior of the polymorphs of d-mannitol. J Pharm Sci. 2000;89:457–68.
26. Pinto JMO, Leão AF, Alves GF, Mendes C, França MT, Fernandes D, et al. New supersaturating drug delivery system as strategy to improve apparent solubility of candesartan cilexetil in biorelevant medium. Pharm Dev Technol. 2020;25:89–99.
27. Riekes MK, Kuminek G, Rauber GS, de Campos CEM, Bortoluzzi AJ, Stulzer HK. HPMC as a potential enhancer of nimodipine biopharmaceutical properties via ball-milled solid dispersions. Carbohydr Polym. 2014;99:474–82.